Integer Quantum Hall Effect

Severin Meng
Proseminar in Theoretical Physics, Departement Physik ETH Zürich

May 28, 2018

Contents

1 The basics of the Integer Quantum Hall Effect

1.1 Introduction

In a two-dimensional electron gas at a very low temperature ($T < 4$ K) subject to a strong perpendicular magnetic field ($B \sim \mathcal{O}(\mathrm{T})$), the electrical conductivity takes on values that are fundamentally different from the predictions of classical physics. The transverse conductivity, also referred to as the *Hall conductivity*, takes quantised values:

$$\sigma_{xy} = \nu \frac{e^2}{2\pi\hbar} \tag{1}$$

where the value ν has been measured to very high precision to be an integer, hence the name *integer quantum Hall effect*. For the discovery of the integer quantum Hall effect, Klaus von Klitzing won the nobel prize in 1985.
The quantisation of the conductivity happens for dirty, many-particle mesoscopic systems. It is a collective quantum effect, like superconductivity. The quantisation is universal in the sense that, to a large extent, it does not depend on microscopic details such as the exact value of the magnetic field, the purity of the sample, the electron mobility etc. It turns out that a topological property of the system is essential to this phenomenon, and surprisingly, disorder is also important.
We are going to look at two seemingly different explanations of the integer quantum Hall effect. In a finite system with edges, one can interpret the Hall current to be carried by excitations near the edge. These *edge states* can also be observed experimentally. They are chiral modes in the sense that they can only carry current in one fixed direction. At the same time, these edge modes are protected in the way that the number of edge modes cannot change under continuous changes in the system. This will be explained in section 2, *The Edge Picture*. For systems with no edges, i.e. bulk systems, one interprets the current to be running within the sample. Using linear response theory, one can derive a formula that guarantees a quantised Hall conductivity for a system fulfilling the right conditions. The system has to have an energy spectrum forming gapped bands, i.e. the electron states have to be periodic in a type of Brillouin zone. This will be explained in section 3, *The Bulk Picture*.
It turns out that both descriptions are two different manifestations of the topological properties of the system. The number of protected edge modes corresponds to a quantised Hall conductivity, and this number is connected to the Chern numbers associated with the gapped energy bands.
This exposition is largely based on the notes of D. Tong [1] and the original literature [2, 3, 4, 5].

1.2 Conductivity and Resistivity in 2D

The Hall effect is observed in two dimensional systems, we therefore work in the (x,y)-plane and only consider two dimensional current densities and electric fields:

$$\mathbf{J} = \begin{pmatrix} J_x \\ J_y \end{pmatrix}, \quad \mathbf{E} = \begin{pmatrix} E_x \\ E_y \end{pmatrix} \tag{2}$$

Ohm's law tells that the conductivity links the electric field to the current density in a linear equation

$$\mathbf{J} = \sigma \mathbf{E} \tag{3}$$

where σ is the conductivity. Its general form is not a scalar but a matrix. For an isotropic sample, the conductivity takes the following form:

$$\sigma = \begin{pmatrix} \sigma_{xx} & \sigma_{xy} \\ -\sigma_{xy} & \sigma_{xx} \end{pmatrix} \tag{4}$$

The resistivity matrix ρ is simply the inverse of σ. A consequence of having a matrix conductivity is that one can have a system with both vanishing longitudinal resistivity and conductivity $\sigma_{xx} = \rho_{xx} = 0$. In the scalar case, a system with $\sigma_{xx} = \sigma = 0$ would be called a perfect insulator, while a system with $\rho_{xx} = \rho = 0$ would be called a perfect conductor. Having both at the same time seems unphysical, however one should not be fooled by this intuition, as in the matrix case, the inverse of the resistivity is given by $\rho_{xx} = \frac{\sigma_{xx}}{\sigma_{xx}^2 + \sigma_{xy}^2}$. The inverse therefore exists even in the case of $\sigma_{xx} = 0$ as long as the transverse conductivity $\sigma_{xy} \neq 0$. A system with $\sigma_{xx} = 0$ is therefore not automatically a perfect insulator in the general case.

1.3 The Classical Hall Effect

Let us first look at the classical Hall effect and then see how it differs from the quantum Hall effect. The classical Hall effect was discovered by Edwin Hall in 1879. The set-up is as follows: Electrons are restricted to move in the 2D (x,y)-plane while a constant magnetic field points in the z-direction. By applying a constant electric field $\mathbf{E}$, a constant current density $\mathbf{J}$ emerges. The Drude model used to describe the motion of a charged particle in this system goes as follows:

$$m\frac{d\mathbf{v}}{dt} = -e\mathbf{E} - e\mathbf{v} \times \mathbf{B} - \frac{m\mathbf{v}}{\tau} \tag{5}$$

where $\mathbf{v}$ is the particle's velocity, $-e\mathbf{E} - e\mathbf{v} \times \mathbf{B}$ is the Lorentz force acting on the particle of charge $-e$ and $\frac{m\mathbf{v}}{\tau}$ is the friction term that models the interaction between the particle and the sample, where τ is the average time between two collision events called *scattering time*. A high value of τ implies a clean sample as collisions occur more rarely. By imposing the equilibrium condition $\frac{d\mathbf{v}}{dt} = 0$ and noting that $\mathbf{J} = -ne\mathbf{v}$ we get the following equation:

$$\begin{pmatrix} 1 & \omega_B\tau \\ -\omega_B\tau & 1 \end{pmatrix} \mathbf{J} = \frac{e^2 n\tau}{m}\mathbf{E} \tag{6}$$

Comparing this with the definition of the resistivity matrix, one finds

$$\rho_{xx} = \frac{m}{ne^2\tau}, \quad \rho_{xy} = \frac{B}{ne}. \tag{7}$$

The longitudinal resistivity is proportional to $\frac{1}{\tau}$, so a high value of the scattering time, i.e. a clean sample, yields a low longitudinal resistivity. The transverse resistivity is

independent of impurities, it depends on the electron density n and linearly on the magnetic field B. One can use this result to measure the electron density of a given sample by measuring its Hall resistivity. The resistivities are plotted as functions of the magnetic field in figure 1.

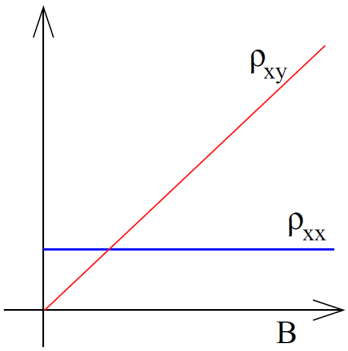

Figure 1: Resistivities of the classical Hall system, as functions of the magnetic field. The blue line shows the longitudinal resistivity ρ_{xx}, it is constant in the magnetic field. The red line denotes the Hall resistivity ρ_{xy}, it depends linearly on the magnetic field. Image reproduced from [1].

1.4 The Results of the Integer Quantum Hall Effect

The experimental set-up for the integer quantum Hall effect is similar to the classical case.
One constructs a two dimensional electron gas from a semiconductor heterostructure, for example a GaAs structure sandwiched in between two AlAs semiconductors. The electrons live in the conduction band of the GaAs, which is lower in energy than the conduction band of the AlAs. They are therefore trapped to live within the layer of GaAs. If one makes this GaAs layer sufficiently thin, the electrons are effectively confined to the two dimensional plane that is the GaAs structure.
One takes this 2D electron gas subject to a constant perpendicular magnetic field. At strong magnetic fields $B \sim \mathcal{O}(\mathrm{T})$ and low Temperatures $T < 4$ K the transverse resistivity ρ_{xy} takes on a plateau form: It is constant over a range of magnetic fields, and jumps to the next plateau once the magnetic field is changed too much. The longitudinal resistivity is zero whenever ρ_{xy} sits on a plateau and spikes when ρ_{xy} changes from one plateau to the next. The experimental results are shown in figure 2. The plateau values of ρ_{xy} are given by the following formula:

$$\rho_{xy} = \frac{2\pi\hbar}{e^2}\frac{1}{\nu}, \quad \nu \in \mathbb{Z} \tag{8}$$

They are independent of the sample details and the precise value of the magnetic field. The integer ν has been measured up to a precision of 1 part in a billion. While ρ_{xy}

takes on a plateau value, the Hall conductivity is simply given by the inverse, namely $\sigma_{xy} = \frac{e^2}{2\pi\hbar}\nu$. In general, there would be a caveat to this: In an experiment, one measures resistance and not resistivity! The two are related via the dimensions of the sample, so the precision of measuring the resistivity is dictated by the precision of the measurement of the sample's dimensions. In 2D however, the transverse Resistance and the transverse resistivity are exactly the same and do not depend on the dimensions of the sample:

$$R_{xy} = \frac{V_y}{I_x} = \frac{LE_y}{LJ_x} = \frac{E_y}{J_x} = -\rho_{xy} \quad (J_y = E_x = 0) \tag{9}$$

Comparing the results from the integer quantum hall effect (figure 2) to the results from the classical model (figure 1), one quickly sees that classical physics does not give us the right answer. We are therefore going to use a quantum mechanical approach to describe the system.

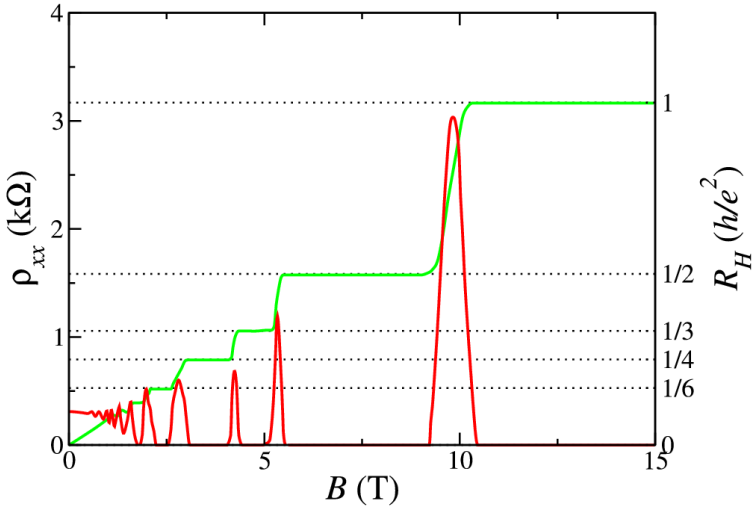

Figure 2: Resistivities of the integer quantum Hall system, as functions of the magnetic field. The red line shows the longitudinal resistivity ρ_{xx}, it is zero as long as ρ_{xy} sits on a plateau level and spikes whenever ρ_{xx} changes from one plateau to the next. The green line denotes the Hall resistivity ρ_{xy}, it takes on a plateau form, i.e. it is constant over a range of magnetic fields. Image reproduced from [6].

1.5 Quantum Treatment

1.5.1 Eigenstates and Eigenvalues

The Hamiltonian for one electron in a 2D system subject to a perpendicular magnetic field $B\hat{\mathbf{z}}$ is

$$H = \frac{1}{2m}(\mathbf{p} + e\mathbf{A})^2 \tag{10}$$

where $\mathbf{A}$ is the vector potential describing the magnetic field: $\nabla \times \mathbf{A} = B\hat{\mathbf{z}}$. Note that the momentum operator $\mathbf{p}$ is the canonical momentum operator and differs from the

kinetic momentum due the magnetic field: $\mathbf{p} = m\dot{\mathbf{x}} - e\mathbf{A}$. Because we are neglecting all electron-electron interaction for this derivation, any many particle state can be constructed from the product of single particle states. By choosing Landau gauge $\mathbf{A} = xB\hat{\mathbf{y}}$ the Hamiltonian becomes

$$H = \frac{1}{2m}(p_x^2 + (p_y + eBx)^2) \tag{11}$$

and is therefore translationally invariant in the y-direction. Consequently, the Hamiltonian commutes with the y-momentum operator p_y, so one can motivate the following Ansatz for the energy eigenstates:

$$\psi_{k_y}(x, y) = e^{ik_y y} f_{k_y}(x) \tag{12}$$

where the plane wave part makes the wavefunction an eigenstate of the y-momentum operator with eigenvalue $\hbar k_y$. By restricting ourselves to the subspace of states with y-momentum $\hbar k_y$, the Hamiltonian can be rewritten as

$$H_{k_y} = \frac{1}{2m}p_x^2 + \frac{m\omega_B^2}{2}(x + k_y l_B^2)^2 \tag{13}$$

where $\omega_B = \frac{eB}{m}$ is the cyclotron frequency and $l_B = \sqrt{\frac{\hbar}{eB}}$ is the magnetic length of the system. But this is the Hamiltonian for a displaced one dimensional harmonic oscillator, centered at $x_0 = -k_y l_B^2$. The energy eigenvalues of the harmonic oscillator are given by

$$E_n = \hbar\omega_B \left(n + \frac{1}{2}\right), \quad n \in \mathbb{N}, \tag{14}$$

they are called Landau levels. The energy eigenfunctions are given by the product of the plane wave and the 1D harmonic oscillator eigenfunctions:

$$\psi_{n,k_y}(x, y) \sim e^{ik_y y} H_n(x + k_y l_B^2) e^{-(x+k_y l_B^2)^2/(2l_B^2)} \tag{15}$$

Part of this product is a Gaussian that localizes the eigenfunction around $x_0 = -k_y l_B^2$ on the scale of the magnetic length l_B, while the eigenfunction is completely extended in the y-direction. The eigenfunctions are labelled by the harmonic oscillator label n and the momentum label k_y. Noting that the energy does not depend on k_y, one would expect a huge degeneracy in the energy levels!

1.5.2 Degeneracy

First let us confine the sample to a finite rectangular region $L_x \times L_y$. In y-direction we have plane waves, so this is equivalent to the particle in a box system in this direction. As a result, the y-momenta become quantised: $k_y = \frac{2\pi}{L_y}\mathbb{Z}$, the distance in y-momentum space between two eingefunctions is therefore $\Delta k_y = \frac{2\pi}{L_y}$. The eigenfunctions are localised in x-direction around $x_0 = -k_y l_B^2$, a logical constraint would be $0 \leq x_0 \leq L_x$, i.e. the

center of the eigenfunction should lie within the sample. Because the center variable x_0 is directly linked to a y-momentum $\hbar k_y$, this condition imposes a constraint on the allowed y-momenta: $-L_x/l_B^2 \leq k_y \leq 0$. The number of states per energy level can now be calculated:

$$N = \frac{L_y}{2\pi} \int_{-L_x/l_B^2}^{0} \mathrm{d}k_y = \frac{eBA}{2\pi\hbar} = \frac{\Phi}{\Phi_0} \tag{16}$$

where $\Phi_0 = \frac{2\pi\hbar}{e}$ is the quantum of flux and $\Phi = AB$ is the total flux through the sample. So the number of states per Landau level is given by the number of flux quanta that go through the sample. One can also define the Landau level filling factor ν as $\nu = \frac{n_e}{n_\Phi} = \frac{n_e 2\pi\hbar}{eB}$ where n_e is the electron density.
The sample is finite and has edges. The eigenstates are localized in one direction, so there should be states that live near the edge of the sample. It turns out that they have interesting properties that help to understand the Quantum Hall effect. These states are called *edge states*.

2 The Edge Picture

2.1 Edge States

The existence of edge states can be motivated classically. In a classical Hall bar with a uniform perpendicular magnetic field, charged particles move in circular motion, the cyclotron orbit. Suppose that our particles are negatively charged and therefore move in counter-clockwise direction. If one places a particle at the right edge of the sample, the particle will do a half-orbit until it collides with the edge. It can't leave the sample and it can also only do counter-clockwise rotational motion, so it will perform another half-orbit, but now it is further down on the edge, see figure 3. The macroscopic effect is a local current on either edge of the sample, with opposing directions, so the net current stays zero.

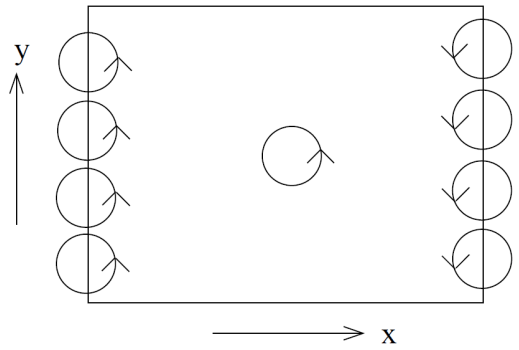

Figure 3: Classical description of the edge states. Particles at the edge of the sample collide with the edge when moving in the cylcotron orbit and result in an edge current. Image reproduced from [1].

Edge states can also be treated quantum mechanically. To model the edge of the sample, one introduces a potential well that rises steeply at the edges, as in figure 4.

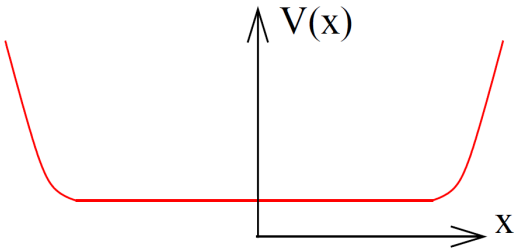

Figure 4: Model of the sample's edges as a steeply rising potential. The red line shows the potential that is due to the boundary of the sample. Image reproduced from [1].

Since the states of the unperturbed system are localised in the x-direction, and by assuming that the potential varies slowly on the scale of the magnetic length, we can Taylor expand the potential around these center positions and drop all the constant terms. Plugging everything back into the Hamiltonian (on the subspace of $\hbar k_y$-momentum states as we have expanded the potential around the corresponding centers) we get

$$H_{k_y} = \frac{p_x^2}{2m} + \frac{1}{2}m\omega_B^2\left(k_y l_B^2 + x\right)^2 + x\frac{\partial V}{\partial x} \tag{17}$$

where $\frac{\partial V}{\partial x}$ is evaluated at $x_0 = -k_y l_B^2$. This Hamiltonian can be rewritten to get another displaced harmonic oscillator plus some extra terms that come from completing the square:

$$H_{k_y} = \frac{p_x^2}{2m} + \frac{1}{2}m\omega_B^2\left(\left(k_y l_B^2 + \frac{\partial V}{\partial x}\frac{1}{m\omega_B^2}\right) + x\right)^2 - \frac{1}{2m\omega_B^2}\left(\frac{\partial V}{\partial x}\right)^2 - k_y l_B^2\frac{\partial V}{\partial x} \tag{18}$$

The extra terms are all constant on the $\hbar k_y$-momentum subspace so they'll transfer over to the energy eigenvalues, while the states will have the same form as the ones found earlier. The resulting energy eigenvalues are

$$E_n(k_y) = \hbar\omega_B\left(n + \frac{1}{2}\right) - \frac{1}{2m\omega_B^2}\left(\frac{\partial V}{\partial x}\right)^2 - k_y l_B^2\frac{\partial V}{\partial x}. \tag{19}$$

They do depend on the y-momentum $\hbar k_y$, so we can calculate a finite group velocity of the wavepackets:

$$v_y = \frac{1}{\hbar}\frac{\partial E}{\partial k_y} = -\frac{1}{eB}\frac{\partial V}{\partial x} \tag{20}$$

By looking again at the potential picture (figure 5) and using the fact that the states are still localised in x-direction, one sees that the states on the right edge propagate in negative y-direction and opposite for the left side.
These edge states are chiral, they can only move in one direction. In a regular wire, there

are electrons that move to the right and ones that move to the left. These right-movers and left-movers can coexist in the same spatial region. Upon reversing time right-movers become left-movers and vice-versa. Since they are in the same spatial region, the system looks the same. For the system here, the right-movers are spatially separated from the left-movers. Time reversal thus returns a system that looks like a mirror-image of the original system, it looks reversed. This asymmetry is due to the presence of the magnetic field.

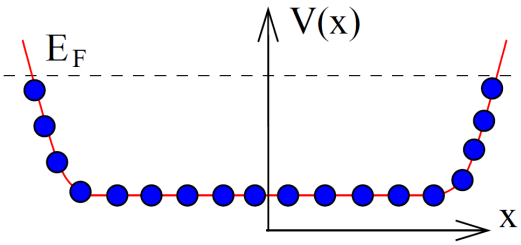

Figure 5: Model of the sample's edges as a steeply rising potential, where the states below the Fermi level E_F are occupied. Blue circles model the centers of the wavefucntions of the occupied states. Image reproduced from [1].

By introducing an electro-chemical potential difference $\Delta\mu$ between the two edges, we can calculate the arising current I_y:

$$I_y = -\frac{e}{L_y}\int \mathrm{d}k_y \frac{L_y}{2\pi} v_y(k_y) = \frac{e}{2\pi l_B^2}\int \mathrm{d}x \frac{1}{eB}\frac{\partial V}{\partial x} = \frac{e}{2\pi\hbar}\Delta\mu \tag{21}$$

where we assumed one completely filled Landau level for the integration. By noting that the Hall voltage V_H across the sample is given by the potential difference, one finds that the Hall conductivity takes the value of the first plateau level:

$$V_H = \frac{\Delta\mu}{e} \Rightarrow \sigma_{xy} = \frac{I_y}{V_H} = \frac{e^2}{2\pi\hbar} \tag{22}$$

The argument can be expanded for multiple filled Landau levels and one will get the corresponding conductivities of the plateaux.
As a side note, the potential introduced before does not have to be flat in the center region, it can be as random as it wants to be (see figure 6) as long as we can make the same arguments for the expansion as before. The resulting Hall current will be the same in any case.

There is another interesting property of the edge states; they are immune to back-scattering by impurities. In the classical picture, defects and impurities scatter incoming electrons into random directions, effectively decreasing the current. Quantum mechanically, the electron always has to occupy a state, so it can only be scattered in one of

the non-populated states. In our system, these states live above the Fermi level, see the empty black circles in figure 6. If an edge state is scattered into a state right above itself, the resulting Hall current will be the same. If it would scatter on to the other side of the sample, the net current would change. However, the width of the sample is macroscopic, so such scattering is highly suppressed. The Hall current carried by the edge states is therefore immune to back-scattering.

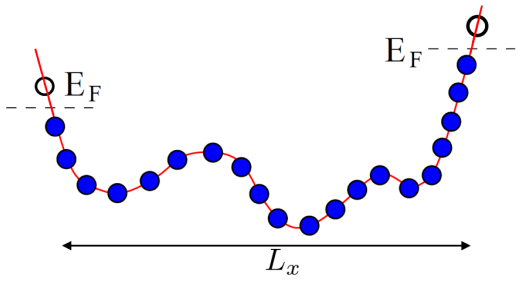

Figure 6: Model of the sample's edges as a steeply rising potential, where the middle part seems random. The empty black circles denote unoccupied states right above the Fermi level. Image reproduced from [1].

The above argument might look convincing, but it does not give any reason as to why the conductivity is stable against change in the magnetic field. To see this, we need something else, we need to add disorder to our system. We will see that disorder is essential for the integer quantum Hall effect.

2.2 The Role of Disorder

Experimentally, there is always disorder in a system. But before we look at the effects of disorder, let us see what happens without it. In the absence of disorder, the Hall system features continuous translational invariance. In the lab frame, the fields are as follows

$$\mathbf{E} = 0, \quad \mathbf{B} = B\hat{\mathbf{e}}_z \tag{23}$$

where the current density $\mathbf{J}$ is zero. Transforming to a Lorentz-boosted reference frame, where the boost is along the y-direction at speed v, the fields become the following:

$$\mathbf{E'} = \gamma v B\hat{\mathbf{e}}_x \approx vB\hat{\mathbf{e}}_x, \quad \mathbf{B'} = \gamma B\hat{\mathbf{e}}_z \approx B\hat{\mathbf{e}}_z \tag{24}$$

where $\gamma \approx 1$ is valid for small v. The transformed current densitiy is

$$\mathbf{J} = nev\hat{\mathbf{e}}_y \tag{25}$$

where the minus sign due to the Lorentz boost cancelled the one coming from the negative charge of the electrons. The electric field expressed in terms of the current density becomes

$$\mathbf{E} = \frac{1}{ne}\mathbf{J} \times \mathbf{B} \Rightarrow \begin{pmatrix} E_x \\ E_y \end{pmatrix} = \frac{B}{ne}\begin{pmatrix} 0 & 1 \\ -1 & 0 \end{pmatrix}\begin{pmatrix} J_x \\ J_y \end{pmatrix} \tag{26}$$

so the resulting resistivities and conductivities are

$$\rho_{xx} = 0, \quad \rho_{xy} = \frac{B}{ne}, \quad \sigma_{xx} = 0, \quad \sigma_{xy} = \frac{ne}{B} \tag{27}$$

which coincide with the classical transverse resistivities.
This Lorentz argument relies purely on translational symmetry, it does not care about any type of mechanics. In reality the result measured is not this classical result, so there has to be something that breaks translational symmetry, and disorder seems to do the job.
Quantum mechanically, the impurities can be modelled by a random potential V that is much smaller than the Landau level spacing: $V \ll \hbar\omega_B$. This potential breaks translational symmetries, so it will lift the degeneracy of the Landau levels, see figure 7. The resulting Landau levels are thus broadened.

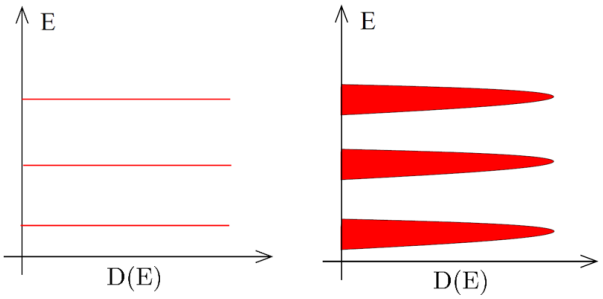

Figure 7: Densitiy of electron states. The left picture is without disorder, showing sharp Landau peaks. The right picture shows broadened peaks due to the effects of disorder. Image reproduced from [1].

Another effect due to disorder is localisation. Figure 8 shows the top-view of a potential landscape on the Hall bar. The lines are equipotential lines, the "+" sign denotes a potential peak and the "-" sign a potential pit. The states derived before have definite energy, they can't change from one equipotential line to another because they can't change their energy. States that live on equipotential lines around peaks and pits are therefore localised, they can't move from one side of the sample to the other and hence can't carry a current. Due to the steeply rising potential at the edge of the sample, extended states are guaranteed to exist at the edges. Using this information, one can add more detail to the picture of the state density, see figure 9. The inner part of the peak contains all the extended states while the shell consists of localised states.

Let us now look at the consequence of localisation. Suppose that our system has a filling factor of $\nu = 1$, i.e. one full Landau level. The Fermi level E_F lies on top of the first peak. Remember the formula for the number of states per Landau level, $N = \frac{BA}{\Phi_0}$. Now we decrease the magnetic field B slightly, so the number of states per Landau level decreases as well. But the number of electrons in the system stays constant, some of

them have to populate states in a higher Landau level. The Fermi level E_F' jumps into the next region of states, which is a region of localised states in the next Landau level, see figure 9. These states however do not carry a current, they can't contribute to the conductivity! The conductivity thus stays constant over a range of magnetic fields, it stays constant as long as the Fermi level lies in a region of localised states, a *mobility gap*. So disorder explains the stability to the magnetic field, it is essential to the whole effect.

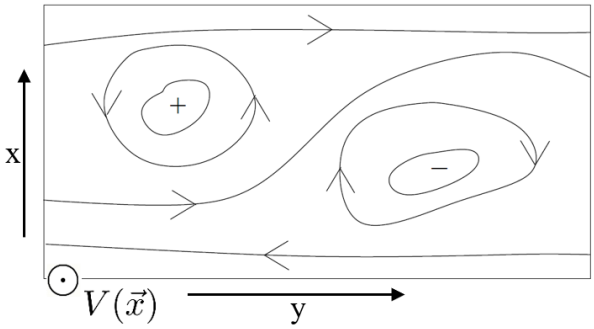

Figure 8: Top view of the potential landscape. The lines are equipotential lines, they form closed loops around peaks ("+" signs) and pits ("-" signs). Image reproduced from [1].

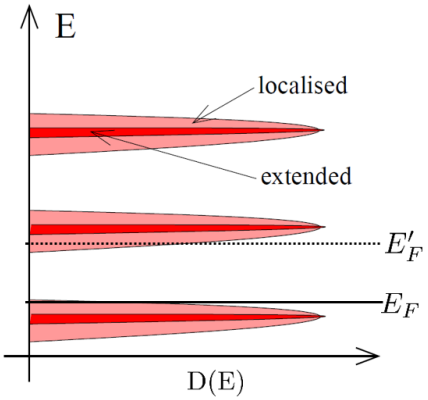

Figure 9: Densitiy of electron states. The outer parts in a Landau peak are localised states, where extended states live in the inner part. The Fermi level E_F before the change in magnetic field lies right at the top of the first Landau level, indicating a filling factor of 1. The Fermi level E_F' after the change in the magnetic field lies in the region of localised states in the second Landau level. Image reproduced from [1].

In the next step we will look at a more sophisticated argument as to why the conductivity is quantized in the values of $\sigma_{xy} = \frac{e^2}{2\pi\hbar}\nu, \quad \nu \in \mathbb{Z}$.

2.3 The Role of Gauge Invariance

The following argument relies on a different geometry that can be achieved by bending the Hall bar into a disk shape, called a Corbino ring, that is shown in figure 10. We are still keeping the constant magnetic field going through the sample. We can introduce a flux Φ that goes through the hole in the disk, without affecting the magnetic field going through the disk surface. Let us assume that this flux can be changed adiabatically, i.e. arbitrarily slowly. Faraday's law then tells us that a change in flux induces an electromotive force $\mathcal{E}$. A radial current I_r would then allow us to calculate the Hall conductivity σ_H of the system, shown by the following equation:

$$\mathcal{E} = -\partial\Phi/\partial t = -\Delta\Phi/T, \quad I_r = \Delta Q_r/T \to \sigma_H = \frac{I_r}{\mathcal{E}} \tag{28}$$

where ΔQ_r is the charge moved radially during the addition of a flux $\Delta\Phi$ during a time T.

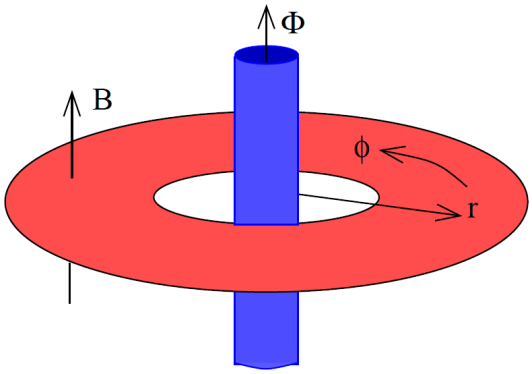

Figure 10: The Corbino geometry, where the states live in the red ring that is penetrated by a uniform magnetic field. The blue tube models the addition of flux through the hole. Image reproduced from [1].

Now we will see that this radial current takes the appropriate values to get the correct Hall conductivity. The system has rotational invariance (we are ignoring disorder for the moment). By choosing the symmetric gauge, this symmetry is still apparent in the Hamiltonian. Remember in the previous derivation of the eigenstates, the Hamiltonian had translational invariance in the y-direction and we found plane waves in said direction. We also found harmonic oscillators in x-direction that were localised. By doing the calculation for this Corbino geometry in the symmetric gauge, one finds again plane waves in azimuthal direction and harmonic oscillators in radial direction:

$$\psi_{m,\nu}(\vec{r}) \sim e^{im\phi} f_\nu(r - r_m) \tag{29}$$

where f_ν is a harmonic oscillator eigenfunction of the level $\nu{+}1$ [2]. The center coordinate r_m is given by $r_m = \sqrt{2l_B^2 m}$ that is now related to the angular momentum $\hbar m$ as opposed

to the x_0 coordinate being related to the y-momentum.
Similar to the Aharonov-Bohm effect [1], adding one flux quantum leaves the system invariant. By adding this amount of flux adiabatically, one finds that the states increase their angular momentum by $\hbar$, they are mapped onto themselves. The center coordinate also increases from r_m to r_{m+1}, so the states effectively move outwards. Because the system comes back to itself after the addition of one flux quantum, the number of electrons in our system stays the same. It started with an integer number of electrons so it ends with an integer number. Therefore exactly one electron per filled Landau level is transferred from the inner to the outer edge. The resulting Hall conductivity takes the values observed in the experiment:

$$\Delta\Phi = \Phi_0 \to \Delta Q_r = -ne, \quad \sigma_H = \frac{ne}{\Phi_0} = n\frac{e^2}{2\pi\hbar}, \tag{30}$$

where n is the number of filled Landau levels. This argument involving the adiabatic change in flux is called the Laughlin flux insertion argument, as Robert B. Laughlin first came up with this idea [3].
We are now going to look at how disorder affects this argument. As seen before, disorder localises the states in the bulk but leaves extended states at the edge. The localised states are not affected by the addition of flux as it can be removed by a gauge transformation. For extended states, this only works if the flux is an integer multiple of magnetic flux quanta, because they have to obey a single-valuedness condition: By changing $\phi \mapsto \phi+2\pi$ the state should remain unchanged. The extended states still undergo spectral flow and map onto themselves under the adiabatic addition of integer number of flux quanta. It is still guaranteed that at least two extended states exist per Landau level, one on either edge. As long as all the extended states in a Landau level are populated, threading one flux quantum results in the radial current and the correct conductivity as we calculated before. The extended states are populated as long as the Fermi level lies in a mobility gap, which is possible due to the existence of disorder. Again, disorder and impurities are responsible for the stability of the Hall conductivity to changes in the magnetic field.

This completes the discussion of the integer quantum Hall effect within the edge picture. Parts of it are heuristic, but the role of gauge invariance hints that there may be a deeper connection. In the next section, we are going to look at the bulk picture and we will find that the integer quantum Hall effect appears as a consequence of a topological property of the Hall system.

3 The Bulk Picture

3.1 The Kubo Formula for Hall Conductivity

Before we can look at the topological property, we need to write the Hall conductivity in a different way, given by the Kubo formula. A full derivation of the Kubo formula can be found in D. Tong's lecture notes about the quantum Hall effect [1]. Here, only a rough sketch of the derivation will be given.
One starts with a multi-particle Hamiltonian H_0 for a generic system that does not include an electric field. We assume that we can solve this system, i.e. we know eigenstates $|m\rangle$ and eigenvalues E_m such that $H_0 |m\rangle = E_m |m\rangle$. We then introduce a weak electric field $\mathbf{E} = -\partial_t \mathbf{A}$ as a perturbation; $\Delta H = -\mathbf{J} \cdot \mathbf{A}$, where $\mathbf{J}$ is the current operator. Our goal is to calculate the expectation value of the current operator $\langle J_x \rangle$ for the system in the non-degenerate ground state $|0\rangle$. It is convenient to work in the interaction picture and expand the expression for $\langle J_x \rangle$ up to linear order in ΔH. Comparing this new expression with Ohm's law $J_x = \sigma_{xx} E_x + \sigma_{xy} E_y$, one can filter out a formula for σ_{xy}. The precise derivation is part of a bigger story called *linear response*, but we are not going deeper into this. As a result, the expression for the Hall conductivity becomes

$$\sigma_{xy} = i \frac{\hbar}{L_x L_y} \sum_{n \neq 0} \frac{\langle 0 \,|\, J_y \,|\, n \rangle \langle n \,|\, J_x \,|\, 0 \rangle - \langle 0 \,|\, J_x \,|\, n \rangle \langle n \,|\, J_y \,|\, 0 \rangle}{(E_n - E_0)^2}. \tag{31}$$

This is the Kubo formula for Hall conductivity. The sum runs over all the excited multi-particle states, inside there are transition amplitudes from excited states over the current operators to the ground state, weighted by the energy difference of these states. So if one can solve the unperturbed system, this formula instantly gives an expression for the Hall conductivity of that system.
In the next section we will see a how a topological property leads to the quantisation of the Hall conductivity.

3.2 Hall System on a Torus

For this section, we have to modify the geometry again. This time, the Hall bar is bent into a torus, which is a rectangle with opposite edges identified. The system is now made fully periodic, all edges have been removed, so there are no more edge states. There is still a homogeneous magnetic field perpendicular to the torus' surface. (Note it is a thought experiment. In an actual experiment, this non-zero magnetic flux through a closed surface would require magnetic monopoles.)

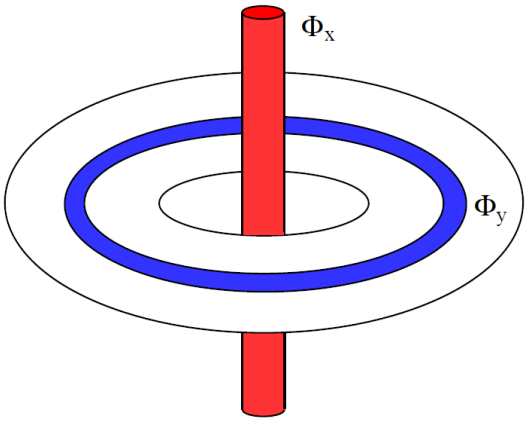

Figure 11: The Hall system on a torus. The red and blue shapes indicate two different fluxes that can be added to the system. Image reproduced from [1].

Now we expand Laughlin's flux threading argument: One can now insert two fluxes, one through either hole of the torus, as in figure 11. The Hamiltonian now depends on these two fluxes, $H = H(\Phi_x, \Phi_y)$. Similar to the previous case, the system's spectrum is only sensitive to the non-integer part of Φ_i/Φ_0, $i \in \{x, y\}$. This time, there are no edges, no electrons transfer from one side to another one. By the addition of one flux quantum, the system comes back to itself fully! Having zero flux is therefore the same as having one flux quantum, which makes the space of parameters of the Hamiltonian periodic:

$$0 \leq \Phi_x < \Phi_0, \quad 0 \leq \Phi_y < \Phi_0 \tag{32}$$

This describes a torus $\mathbf{T}^2_\Phi$, the parameter space of our system is toroidal. Let us now calculate the system's Hall conductivity.
Let H_0 describe the unperturbed system. Treat the addition of flux as a perturbation ΔH given by

$$\Delta H = -\sum_{i=x,y} \frac{J_i \Phi_i}{L_i} \tag{33}$$

where L_x and L_y are the dimensions of the system. One can now use first order perturbation theory to calculate the many particle ground state of the perturbed system:

$$|\psi_0'\rangle = |\psi_0\rangle + \sum_{n \neq \psi_0} \frac{\langle n \,|\, \Delta H \,|\, \psi_0 \rangle}{E_n - E_0} |n\rangle \tag{34}$$

where $|\psi_0\rangle$ is the non-degenerate ground state of the unperturbed system. Consider now infinitesimal changes in flux and see how the state changes:

$$\left| \frac{\partial \psi_0'}{\partial \Phi_i} \right\rangle = -\frac{1}{L_i} \sum_{n \neq \psi_0} \frac{\langle n | J_i | \psi_0 \rangle}{E_n - E_0} |n\rangle \tag{35}$$

The elements in this summation look similar to the Kubo formula, eq. (31)! One can actually rewrite the Kubo formula (and therefore the Hall conductivity) in terms of these states:

$$\sigma_{xy} = i\hbar \left[\left\langle \frac{\partial \psi_0'}{\partial \Phi_y} \middle| \frac{\partial \psi_0'}{\partial \Phi_x} \right\rangle - \left\langle \frac{\partial \psi_0'}{\partial \Phi_x} \middle| \frac{\partial \psi_0'}{\partial \Phi_y} \right\rangle \right] \tag{36}$$

This expression can be rewritten by pulling out one derivative for each one of the brakets, becoming

$$\sigma_{xy} = i\hbar \left[\frac{\partial}{\partial \Phi_y} \left\langle \psi_0' \middle| \frac{\partial \psi_0'}{\partial \Phi_x} \right\rangle - \frac{\partial}{\partial \Phi_x} \left\langle \psi_0' \middle| \frac{\partial \psi_0'}{\partial \Phi_y} \right\rangle \right]. \tag{37}$$

This however looks similar to the field strength of a Berry connection. Let us first parameterise the torus using the dimensionless variables

$$\theta_i = \frac{2\pi \Phi_i}{\Phi_0}, \quad \theta_i \in [0, 2\pi). \tag{38}$$

Now, the Berry connection [1] is defined as

$$\mathcal{A}_i(\Phi) = -i \left\langle \psi_0' \middle| \frac{\partial}{\partial \theta_i} \middle| \psi_0' \right\rangle. \tag{39}$$

The field strength, or curvature of the Berry connection is the curl of the connection:

$$\mathcal{F}_{xy} = \frac{\partial \mathcal{A}_x}{\partial \theta_y} - \frac{\partial \mathcal{A}_y}{\partial \theta_x} = -i \left[\frac{\partial}{\partial \theta_y} \left\langle \psi_0' \middle| \frac{\partial \psi_0'}{\partial \theta_x} \right\rangle - \frac{\partial}{\partial \theta_x} \left\langle \psi_0' \middle| \frac{\partial \psi_0'}{\partial \theta_y} \right\rangle \right] \tag{40}$$

This term looks pretty much the same as our expression for the conductivity, eq (37). The difference that in one case, the derivatives are with respect to θ_i instead of Φ_i, gives the right constants. As a result, the conductivity is given by the curvature:

$$\sigma_{xy} = -\frac{e^2}{\hbar} \mathcal{F}_{xy} \tag{41}$$

This does not tell us much yet. However if one averages this expression over all fluxes in the toroidal parameter space $\mathbf{T}^2_\Phi$, one gets a more interesting result:

$$\sigma_{xy} = -\frac{e^2}{2\pi\hbar} \int_{\mathbf{T}^2_\Phi} \frac{\mathrm{d}\theta}{2\pi} \mathcal{F}_{xy} = -\frac{e^2}{2\pi\hbar} C \tag{42}$$

where

$$\int_{\mathbf{T}^2_\Phi} \frac{\mathrm{d}\theta}{2\pi} \mathcal{F}_{xy} = C \in \mathbb{Z} \tag{43}$$

is the first Chern number, and it is always an integer [7].
This result is the topological argument we have been looking for. The Hall conductivity is a Chern number, it can't continuously change. It is therefore invariant under small changes of the Hamiltonian, which would result in small changes of the Berry curvature. One would always expect a graph of Chern numbers to form plateaux. Large

deformations correspond to energy level crossings, and our non-degeneracy assumption breaks down. This situation describes a transition between two Chern numbers, i.e. two plateau levels in the conductivity.
We have seen that for a system with continuous translational symmetry, a toroidal parameter space led to the desired quantisation. However, we haven't seen a reason as to why one should average the conductivity over the parameter space, and I do not know one either. It turns out that if one looks at particles on a lattice, the integral appears naturally, without taking any averages. Such a system was used originally to measure the quantum Hall effect. It only features *discrete* translational invariance, so one might expect some things to go wrong. In the next sections, we are going to look at this more closely.

3.3 Particles on a Lattice

A lattice has a discrete periodicity given by the lattice vectors $\mathbf{r_n}$, and so does the corresponding lattice potential. The energy spectrum of such a system forms bands. Due to Bloch's theorem, we know that the wavefunctions in each band can be written in the Bloch form as

$$\psi_{\mathbf{k}}(\mathbf{r}) = e^{i\mathbf{k}\cdot\mathbf{r}}u_{\mathbf{k}}(\mathbf{r}), \quad u_{\mathbf{k}}(\mathbf{r}) = u_{\mathbf{k}}(\mathbf{r}+\mathbf{r_n}), \quad \psi_{\mathbf{k}+\mathbf{G}}(\mathbf{r}) = \psi_{\mathbf{k}}(\mathbf{r}) \tag{44}$$

where $\mathbf{k}$ is the lattice momentum and $\mathbf{G}$ is a reciprocal lattice vector. Most importantly, the wavefunction is periodic in the first Brillouin zone. For a rectangular lattice with lattice constants a and b, the Brillouin zone is rectangular as well. But a periodic rectangle is a torus, so our wavefunction is periodic on a toroidal space $\mathbf{T}^2$ of lattice momenta:

$$-\frac{\pi}{a} < k_x \leq \frac{\pi}{a}, \quad -\frac{\pi}{b} < k_y \leq \frac{\pi}{b} \tag{45}$$

Let us now assume that the Fermi level E_F lies in a gap between two energy bands, meaning that all the bands below the Fermi level are completely filled, and all the bands above are completely unoccupied. The Hamiltonian of such a system can be rewritten using Bloch's theorem:

$$H\left|\psi_k\right\rangle = E_k\left|\psi_k\right\rangle \Rightarrow \widetilde{H}(\mathbf{k})\left|u_{\mathbf{k}}\right\rangle = E_{\mathbf{k}}\left|u_{\mathbf{k}}\right\rangle \text{ with } \widetilde{H}(\mathbf{k}) = e^{-i\mathbf{k}\cdot\mathbf{x}}He^{i\mathbf{k}\cdot\mathbf{x}} \tag{46}$$

The current operator is now given by

$$\mathbf{J} = \frac{e}{\hbar}\frac{\partial\widetilde{H}}{\partial\mathbf{k}} \tag{47}$$

which is analogous to the more conventional $\mathbf{J} = -e\dot{\mathbf{x}}$. The Kubo formula we have seen in section 3.1 can be rewritten in terms of single particle states. This is because all electron-electron interactions are neglected, so a multi-particle state is just a product of all the single-particle states. For states living in discrete energy bands with continuous lattice momenta, the Kubo formula becomes

$$\sigma_{xy} = i\hbar \sum_{E_\alpha < E_F < E_\beta} \int_{\mathbf{T}^2} \frac{d^2k}{(2\pi)^2} \frac{\langle u^\alpha_{\mathbf{k}}|J_y|u^\beta_{\mathbf{k}}\rangle\langle u^\beta_{\mathbf{k}}|J_x|u^\alpha_{\mathbf{k}}\rangle - \langle u^\alpha_{\mathbf{k}}|J_x|u^\alpha_{\mathbf{k}}\rangle\langle u^\alpha_{\mathbf{k}}|J_y|u^\alpha_{\mathbf{k}}\rangle}{\left(E_\beta(\mathbf{k}) - E_\alpha(\mathbf{k})\right)^2} \tag{48}$$

where the sum runs over all the energy bands and the integral runs over all the continuous lattice momenta in each band. By plugging the Ansatz for the current operator (47) into this Kubo formula, one gets

$$\sigma_{xy} = \frac{ie^2}{2\pi\hbar} \sum_{\alpha} \int_{\mathbf{T}^2} \frac{d^2k}{2\pi} \left[\langle \partial_y u^{\alpha}_{\mathbf{k}} | \partial_x u^{\alpha}_{\mathbf{k}} \rangle - \langle \partial_x u^{\alpha}_{\mathbf{k}} | \partial_y u^{\alpha}_{\mathbf{k}} \rangle \right]. \tag{49}$$

Let us now look at the following $U(1)$ Berry connection, defined over $\mathbf{T}^2$:

$$\mathcal{A}^{\alpha}_i(\mathbf{k}) = -i \left\langle u^{\alpha}_{\mathbf{k}} \middle| \frac{\partial}{\partial k^i} \middle| u^{\alpha}_{\mathbf{k}} \right\rangle \tag{50}$$

The field strength associated to this connection is

$$\mathcal{F}^{\alpha}_{xy} = \frac{\partial \mathcal{A}^{\alpha}_x}{\partial k_y} - \frac{\partial \mathcal{A}^{\alpha}_y}{\partial k_x} = -i \left[\left\langle \frac{\partial u^{\alpha}}{\partial k_y} \middle| \frac{\partial u^{\alpha}}{\partial k_x} \right\rangle - \left\langle \frac{\partial u^{\alpha}}{\partial k_x} \middle| \frac{\partial u^{\alpha}}{\partial k_y} \right\rangle \right]. \tag{51}$$

By integrating this field strength over the Brillouin zone $\mathbf{T}^2$, one obtains the first Chern number,

$$C_{\alpha} = \int_{\mathbf{T}^2} \frac{\mathrm{d}^2k}{2\pi} \mathcal{F}^{\alpha}_{xy}. \tag{52}$$

By comparing equations (51) and (52) with the expression for the Hall conductivity (49), we get

$$\sigma_{xy} = -\frac{e^2}{2\pi\hbar} \sum_{\alpha} C_{\alpha}, \quad C_{\alpha} \in \mathbb{Z}. \tag{53}$$

This is the TKNN formula, named after Thouless, Kohmoto, Nightingale and Nijs, which are the people that came up with it [4]. It tells us that each isolated, filled band (labelled by α) contributes an integer part C_{α} to the Hall conductivity of the system. The set of C_{α} is sometimes called the *TKNN integers*. We have attributed this set of integers to a Hamiltonian, they define the Hall conductivity of the corresponding system. Similar to the case in section 3.2, this formula states that the Hall conductivity is a topological invariant of the system. It is robust to small changes of the system as it can't change continuously.
We are going to see a more precise formulation of this statement in the end. Let us now look at an example, giving a hint at this more precise formulation.

3.3.1 Example: The Chern Insulator

The system we are looking at has two distinct energy bands and the Fermi level lies between them, meaning the system is insulating. Even though there is no magnetic field, this system can have a non-zero Chern number, hence the name *Chern insulator*. The system in $\mathbf{k}$-space is modelled by a two-state Hamiltonian in the most general form,

$$\widetilde{H}(\mathbf{k}) = \vec{E}(\mathbf{k}) \cdot \vec{\sigma} + \epsilon(\mathbf{k}) \mathbb{1} \tag{54}$$

where $\vec{\sigma}$ are the Pauli matrices. The energy eigenvalues corresponding to this system are given by $\epsilon(\mathbf{k}) \pm |\vec{E}(\mathbf{k})|$. The fact that the system is insulating translates into $\vec{E}(\mathbf{k}) \neq 0 \, \forall \, \mathbf{k}$. One can therefore define the following three-vector $\vec{n}$:

$$\vec{n}(\mathbf{k}) = \frac{\vec{E}(\mathbf{k})}{|\vec{E}(\mathbf{k})|} \tag{55}$$

This vector has unit length, but varies continuously as $\mathbf{k}$ varies over the Brillouin zone, it is a mapping from the torus to the (Bloch-) sphere:

$$\vec{n} : \mathbf{T}^2 \to \mathbf{S}^2 \tag{56}$$

The Chern number associated with this system is given by

$$C = \frac{1}{4\pi} \int_{\mathbf{T}^2} \mathrm{d}^2 k \; \vec{n} \cdot \left(\frac{\partial \vec{n}}{\partial k_x} \times \frac{\partial \vec{n}}{\partial k_y} \right) \tag{57}$$

which can be interpreted as counting how many times the torus wraps around the sphere.

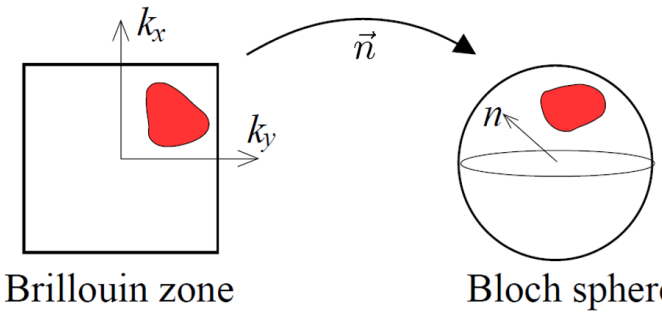

Figure 12: The three-vector $\vec{n}$ is a mapping between the toroidal Brillouin zone and the Bloch sphere. Image reproduced from [1].

Let us now try to classify the maps from the torus to the sphere. In this case, there is a subtlety: maps from the torus to the sphere are isomorphic to maps from sphere to sphere. These maps are classified by the second homotopy group of the sphere, $\pi_2(S^2)$. It turns out that this group is isomorphic to the set of integers,

$$\pi_2(S^2) = \mathbb{Z}. \tag{58}$$

Since our Hamiltonian is basically $\vec{E}(\mathbf{k})$ which is represented by the sphere S^2, this result tells us that any two systems that are deformable into each other (homotopic) have the same Chern number and hence the same Hall conductivity! A system with zero Hall conductivity therefore can't be continuously transformed into a system with finite Hall conductivity because their Hamiltonians live in different homotopy classes. This again explains the robustness of the Hall-state, but just for this two-state system.
This example is a special case of a more general thing. There is a theorem stating that

two maps from the Brillouin zone to the space of gapped hermitian matrices (Hamiltonians) are homotopic if and only if the they both have the same TKNN integers, and therefore have the same Hall conductivity, see [5]. We will come back to this again in section 4.
In the next section we are going to look how things change when we introduce a magnetic field. It is not obvious that the Brillouin zone survives this addition, so we might want to check if the TKNN formula is still applicable.

3.4 Particles on a Lattice in a Magnetic Field

So far we haven't included a magnetic field into our discussion about particles on a lattice. In the experiment, this has been done, and from the edge picture we know that a magnetic field is crucial to the effect. The main goal of this treatment is to find a zone where the states of the system are periodic, we want to find an analogue to the Brillouin zone. If we have that, one can simply apply the TKNN formula. It is not obvious that there exists such a magnetic Brillouin zone as the Hamiltonian loses the discrete translational invariance of the lattice due to the vector potential arising from the magnetic field.
Let us work in the tight-binding approximation and assume a square lattice with lattice constant a. One can also find a Brillouin zone when working with a weak potential and a non-square lattice, see [4]. In the tight-binding approximation, the states are localised around the lattice points. These position eigenstates $|\mathbf{x}\rangle$ are discrete, they are restricted to $\mathbf{x} = a(m, n)$ with $m, n \in \mathbb{Z}$. The Hamiltonian is discrete as well. For this approximation of a strong potential, the Hamiltonian allows states to hop from one lattice site to an adjacent one. It is given by

$$H = -t \sum_{\mathbf{x}} \sum_{j=1,2} |\mathbf{x}\rangle \langle \mathbf{x} + \mathbf{e}_j| - t^* \sum_{\mathbf{x}} \sum_{j=1,2} |\mathbf{x} + \mathbf{e}_j\rangle \langle \mathbf{x}| \tag{59}$$

with $\mathbf{e}_1 = (a, 0)$, $\mathbf{e}_2 = (0, a)$ and t being the probability amplitude for hopping to occur. The on-site energy has been set to zero, it is just an additive constant to the Hamiltonian. Now we can add a magnetic field to the system,

$$B\hat{\mathbf{z}} = \nabla \times \mathbf{A}. \tag{60}$$

Intuitively, a vector potential is part of the canonical momentum $\mathbf{p}$. Canonical momentum is the rate at which the phase of a state changes, per unit length. For our set of discrete states, this length is fixed at a. So the change in the Hamiltonian is just a phase, its new form is

$$H = -t \sum_{\mathbf{x}} \sum_{j=1,2} |\mathbf{x}\rangle \, e^{-iaeA_j(\mathbf{x})/\hbar} \langle \mathbf{x} + \mathbf{e}_j| + \text{h.c.}, \tag{61}$$

which has no discrete translational invariance anymore. This Hamiltonian should better be compatible with the Aharonov-Bohm effect, and indeed it is. Let us take a state and move it once around a unit cell (see figure 13), it will pick up a phase of $e^{-i\gamma}$. This γ

can be calculated from the form of the Hamiltonian, and it is

$$\gamma = \frac{ea}{\hbar}\left(A_1(x) + A_2(x+e_1) - A_1(x+e_2) - A_2(x)\right) \approx \frac{ea}{\hbar}\left(\frac{\partial A_2}{\partial x^1} - \frac{\partial A1}{\partial x^2}\right) \tag{62}$$

where in the second step, we have approximated finite differences with actual derivatives (remember our space coordinate is discretised). But the expression in the bracket is just the curl of the vector potential, so

$$\gamma \approx \frac{ea}{\hbar}\left(\frac{\partial A_2}{\partial x^1} - \frac{\partial A1}{\partial x^2}\right) = \frac{ea^2 B}{\hbar} \tag{63}$$

where $a^2 B$ is the magnetic flux through the unit cell, so this really is the Aharonov-Bohm phase.

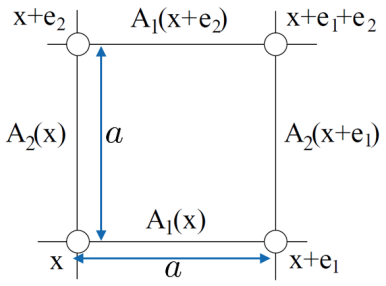

Figure 13: Schematic view of the square lattice. A state moving along a lattice site picks up a phase proportional to the vector potentials written above each line. Image reproduced from [1].

Now that we have a Hamiltonian, we want to find eigenstates and eigenvalues. Our goal is to find operators that commute with the Hamiltonian and then to find a common set of eigenstates. Let us define the modified magnetic translation operators:

$$\widetilde{T}_j = \sum_{\mathbf{x}} |\mathbf{x}\rangle\, e^{-iea\widetilde{A}_j(\mathbf{x})/\hbar}\, \langle \mathbf{x} + \mathbf{e}_j| \tag{64}$$

The $\widetilde{A}_j$ is not the same vector potential as before, but it fulfils $\partial_k \widetilde{A}_j = \partial_j A_k$. These operators have the following commutation relations:

$$[H, \widetilde{T}_j] = 0, \quad \widetilde{T}_2\widetilde{T}_1 = e^{ie\Phi/\hbar}\widetilde{T}_1\widetilde{T}_2 \tag{65}$$

The first commutation relation can be seen by introducing the usual magnetic translation operator (which replaces $\widetilde{A}_j$ by A_j). The Hamiltonian is then given by a superposition of these operators, and they commute with their modified counterparts. The second relation we don't like quite as much yet. It would be nicer if $[\widetilde{T}_1, \widetilde{T}_2]$ were zero as well, because in that case one could find simultaneous eigenstates of all three operators. For this to happen we need to take the flux per unit cell to be a rational multiple of the flux

quantum: $Ba^2 = \Phi = \frac{p}{q}\Phi_0$, with p, q integers that are relatively prime. Then, one can rise the modified magnetic translation operators to an appropriate power and one gets

$$[\widetilde{T}_1^{n_1}, \widetilde{T}_2^{n_2}] = 0 \tag{66}$$

whenever $\frac{p}{q} n_1 n_2 \in \mathbb{Z}$, in particular for $n_1 = q, n_2 = 1$. Of course they still commute with the Hamiltonian. So a set of commuting operators is given by H, $\widetilde{T}_1^q$, $\widetilde{T}_2$ and we can now move on to the eigenstates. Let us label these states by their magnetic lattice momentum $\mathbf{k}$:

$$|\mathbf{k}\rangle\,, \mathbf{k} = (k_1, k_2) \tag{67}$$

The eigenvalue equations then become

$$H\,|\mathbf{k}\rangle = E(\mathbf{k})\,|\mathbf{k}\rangle\,, \quad \widetilde{T}_1^q\,|\mathbf{k}\rangle = e^{iqk_1 a}\,|\mathbf{k}\rangle\,, \quad \widetilde{T}_2\,|\mathbf{k}\rangle = e^{ik_2 a}\,|\mathbf{k}\rangle\,. \tag{68}$$

We see that the k_i are again periodic:

$$-\frac{\pi}{qa} < k_1 \leq \frac{\pi}{qa} \text{ and } -\frac{\pi}{a} < k_2 \leq \frac{\pi}{a} \tag{69}$$

The zone of periodicity is called the magnetic Brillouin zone, and it again forms a Torus $\mathbf{T}^2$! It is smaller by a factor of q compared to the conventional Brillouin zone. The corresponding unit cell (enlarged by a factor of q) contains p magnetic flux quanta. Finding the Brillouin zone hence boils down to finding a unit cell containing an integer number of magnetic flux quanta! The number of states per magnetic Brillouin zone is given by $L_1 L_2/qa^2$. This suggests that the energy spectrum decomposes into q bands. Now we look at the degeneracy of the states. Let us pay closer attention to the state $\widetilde{T}_1\,|\mathbf{k}\rangle$ which is not an eigenstate of $\widetilde{T}_1$. From the calculations before, we know that $\widetilde{T}_1$ commutes with the Hamiltonian, $[H, \widetilde{T}_1] = 0$. We have

$$H\widetilde{T}_1\,|\mathbf{k}\rangle = E(\mathbf{k})\,|\mathbf{k}\rangle\,, \quad \widetilde{T}_2\widetilde{T}_1\,|\mathbf{k}\rangle = e^{ie\Phi}\widetilde{T}_1\widetilde{T}_2\,|\mathbf{k}\rangle = e^{i(2\pi p/q + k_2 a)}\widetilde{T}_1\,|\mathbf{k}\rangle\,. \tag{70}$$

From equation (68) we know that $\widetilde{T}_2\,|\mathbf{k}\rangle = e^{ik_2 a}\,|\mathbf{k}\rangle$, so

$$\widetilde{T}_1\,|\mathbf{k}\rangle \sim |(k_1, k_2 + 2\pi p/qa)\rangle \tag{71}$$

and it also has the same energy as $|(k_1, k_2)\rangle$. This results in a q-fold degeneracy in a given band. One can now go on and calculate the energy eigenvalues and the Chern numbers. However, one might expect to run into some issues, as each isolated band has to contribute an integer number of $\frac{e^2}{2\pi\hbar}$ to the Hall conductivity, and the number of bands q can become arbitrarily large by changing the magnetic flux Φ by an arbitrarily small amount. Also, if the flux is given by an irrational multiple of Φ_0, the above calculation doesn't work out and the spectrum of the Hamiltonian forms a Cantor set. But the experiment shows the conductivity to remain constant over a range of magnetic flux, no rapid behaviour is observed. Nontheless, the calculation works out, but it is not given here as it is rather complicated. It can be found in the original TKNN paper [4] and in the book *Field Theories of Condensed Matter Physics* by Fradkin [8].

Now we have all that we need to apply the TKNN formula (53): There exists a toroidal Brillouin zone and the spectrum decomposes into bands. As a result, the system has a quantised Hall conductivity. So we found the quantised conductivity for the Hall system in a picture without edges! This concludes the discussion of the integer quantum Hall effect within the bulk picture.

4 Conclusion

Now that we have found the quantised conductivity in the lattice model, one might ask what exactly the topological property of the Hall system is. There is a theorem [5] that answers this question, it was briefly mentioned in section 3.3.1. It goes as follows: Let $H_1(\mathbf{k}), H_1(\mathbf{k})$: $\mathbf{T}^2 \to$ [space of Hamiltonian matrices] be two maps from the (magnetic) Brillouin zone (which is toroidal) to the space of gapped, periodic, hermitian matrices, i.e. Hamiltonians that describe the system, the band structure. Then, these two maps are continuously deformable into each other (homotopic) if and only if they have the same TKNN integers. Remember the TKNN formula giving the Hall conductivity for such a system,

$$\sigma_{xy} = -\frac{e^2}{2\pi\hbar} \sum_{\alpha} C_\alpha, \quad C_\alpha \in \mathbb{Z}. \tag{72}$$

This theorem tells us, that if two systems are continuously deformable into each other, they have the same Hall conductivity. If they have different Chern numbers (and hence a different conductivity), they are not deformable into each other, they live in different homotopy classes. It also shows us that the topological property lies in the connection between the Brillouin zone and the band structure (which is $H(\mathbf{k})$).
At the same time, we found a quantised Hall conductivity in the edge picture. These edge modes are the counterpart to the quantised conductivity, their robustness is due to this topological property of the Hamiltonian. The topology is physically manifest in the number of protected edge modes of the system. The edge modes exist because of the topological indices of the system, the TKNN integers. This correspondence is also known as the *bulk-edge correspondence*.

References

[1] D. Tong, "The Quantum Hall Effect", arXiv:1606.06687.

[2] B.I. Halperin, "Quantized Hall conductance, current-carrying edge states, and the existence of extended states in a two-dimensional disordered potential", Phys. Rev. B 25, 2185 (1982).

[3] R.B. Laughlin, "Quantized Hall conductivity in two dimensions", Phys. Rev. B 23, 5632 (1981).

[4] D.J. Thouless, M. Kohmoto, M. Nightingale, M. den Nijs, "Quantized Hall Conductance in a Two-Dimensional Periodic Potential", Phys. Rev. Lett. 49, 405 (1982).

[5] J.E. Avron, R. Seiler, B. Simon, "Homotopy and Quantization in Condensed Matter Physics", Phys. Rev. Lett. 51, 51 (1983).

[6] The University of Manchester, "Advanced Quantum Mechanics 2" [Online], http://oer.physics.manchester.ac.uk/AQM2/Notes/Notes-4.4.html

[7] N. Manton, P. Sutcliffe, "Topological Solitons", Cambridge University Press (2004).

[8] E. Fradkin, "Field Theories of Condensed Matter Physics", University of Illinois (2013).